PHYSICAL REVIEW B VOLUME 26, NUMBER 10 15 NOVEMBER 1982

Elastic behavior under pressure of the vacancy compounds $Hg_5Ga_2\square Te_8$, $Hg_3In_2\square Te_6$, and $HgIn_2\square Te_4$

Tu Hailing, G. A. Saunders, and W. A. Lambson
School of Physics, University of Bath, Claverton Down, Bath, BA2 7AY, England

(Received 29 January 1982)

$Hg_5Ga_2\square Te_8$, $Hg_3In_2\square Te_6$, and $HgIn_2\square Te_4$ are semiconducting vacancy compounds which may be thought of as having tetrahedrally coordinated structures with a sublattice of unfilled sites. Measurements of the hydrostatic pressure dependences of ultrasonic-wave transit times in single crystals of these compounds have been made and used to obtain the pressure derivatives of the elastic-stiffness constants. The elastic behavior of these compounds under pressure is compared with that of the "parent" zinc-blende-structure compound HgTe. It is found that the compression $V(P)/V_0$ of the vacancy compounds becomes larger as the proportion of empty cation sites is increased. The effect of hydrostatic pressure on the gradient of the acoustic-phonon branches at the Brillouin-zone center is discussed in terms of the mode-Grüneisen gammas. The presence of the sited vacancies is shown to inhibit the softening of shear modes characteristic of HgTe and related zinc-blende-structure compounds. Thus, for vacancy compounds, the shear-to-bulk modulus ratios $\frac{1}{2}(C_{11}-C_{12})/B$ and C_{44}/B, or the ratio β/α of the bond-bending to -stretching force constants, do not reach the limiting values for crystal stability and the densification transition until much higher pressures than that found for HgTe.

I. INTRODUCTION

$Hg_3In_2\square Te_6$, $Hg_5Ga_2\square Te_8$, and $HgIn_2\square Te_4$ are vacancy compounds which can be considered to have tetrahedrally coordinated structures except that some of the tetrahedral sites, comprising an ordered sublattice, are empty. If the vacancy is treated as an atom of zero valency, then the Grimm-Sommerfeld rule—that there is an average of four valence electrons per atom—holds.[1] The presence of the ordered array of vacancies leads to a number of physical phenomena peculiar to the lattice-dynamical behavior of such compounds, including breathing modes in which the four anions neighboring a vacancy vibrate symmetrically in the direction of the vacancy center. Breathing modes are responsible for both multiphonon effects and strong Raman scattering in ordered vacancy compounds.[2–4] Recently Miller, MacKinnon, and Weaire[4] gave a comparative review of the ternary semiconductors, including the chalcopyrites and vacancy compounds with a discussion of the way in which the band structure and lattice-dynamical behavior of these compounds derives from their structures.

The influence of an ordered array of vacancies on the elastic behavior of tetrahedrally bonded materials has been examined previously[5,6] by measurements of the elastic constants of a series of such compounds: HgTe, $Hg_5In_2\square Te_8$, $Hg_3In_2\square Te_6$, $HgIn_2\square Te_4$. These compounds can be considered as being derived from the parent zinc-blende-structure compound HgTe by introduction of $In_2\square Te_3$ in simple ratio quantities. In this series the concentration of vacant cation sites increases from zero in HgTe, to one in eight for $Hg_5In_2\square Te_8$, one in six for $Hg_3In_2\square Te_6$, and one in four for $HgIn_2\square Te_4$. $Hg_5In_2\square Te_8$ and $Hg_3In_2\square Te_6$ are cubic with ordered zinc-blende superlattices, while $HgIn_2\square Te_4$ is tetragonal ($c/a=2.0$) but is pseudocubic in its elastic behavior. To compare the elastic properties of zinc-blende compounds with different nearest-neighbor interionic separations d, Keyes[7] reduced the elastic constants to a set of dimensionless parameters using a constant C_0 given by e^2/d^4 ($=256e^2/9a_0^4$), where e is the electronic charge and a_0 is the length of the side of a zinc-blende cube. The reduced bulk modulus B/C_0 of the mercury indium tellurides is approximately linearly dependent upon the percentage of vacant cation sites: Each vacant site decreases the reduced bulk modulus by the same amount.[5,6] Elastic-constant measurements made on two members $Hg_3Ga_2\square Te_6$ and $Hg_5Ga_2\square Te_8$ of the equivalent gallium-compound series showed that the bulk moduli are similar to the isomorphous indium compounds, a finding which reinforces the suggestion that the ordered array of vacancies dominates the elastic behavior of the vacancy compounds.

The effects of hydrostatic pressure on these vacancy compounds should be interesting, yet at present few pressure studies have been made. The variation with pressure of electrical properties has shown that $Hg_5In_2\square Te_8$ and $Hg_3In_2\square Te_6$ transform at about 42×10^8 and 46×10^8 Pa,[8] respectively, to rocksalt phases.[9] Transformation under high pressures to a denser form, which can be one of the related white-tin, rocksalt, or cinnabar structures, is a common feature of the tetrahedrally bonded semiconductors. This type of transition is closely linked with softening of transverse-acoustic (TA) phonon modes. Measurements of the elastic constants of the zinc-blende compounds HgTe (Ref. 10) and HgSe (Ref. 11) up to their respective transition pressures P_t ($16-18\times 10^8$ and 9.5×10^8 Pa) have shown that in both crystals the shear stiffnesses $\frac{1}{2}(C_{11}-C_{12})$ and C_{44} decrease as the pressure is increased: Long-wavelength zone-center TA phonons soften under pressure. Similar mode softening has been observed in the ternary compound semiconductor $CdGeAs_2$ which has the chalcopyrite structure.[12] In the present work the effects of hydrostatic pressure on ultrasonic-wave velocities and thus of the pressure derivatives of the elastic constants of $Hg_3In_2\square Te_6$, $Hg_5Ga_2\square Te_8$, and $HgIn_2\square Te_4$ have been studied. One objective of these experiments, the first of their kind on vacancy compounds, has been to answer the question: What is the influence of sited vacancies on TA-mode softening at the long-wavelength limit? This question is answered by examination of the pressure derivatives of the elastic constants and the acoustic-mode Grüneisen parameters.

II. EXPERIMENTAL PROCEDURE AND RESULTS

Single crystals of the cubic compounds $Hg_3In_2\square Te_6$ and $Hg_5Ga_2\square Te_8$ and the tetragonal compound $HgIn_2\square Te_4$ were grown by a modified Bridgman technique: The ultrasonic specimens were those used in the earlier elastic-constant determinations.[5,6] The elastic constants of compounds in the mercury indium telluride and mercury gallium telluride compound series measured at 77 K are collected in Table I, which also includes data for another ternary semiconductor: the chalcopyrite $CdGeAs_2$.[12]

The room-temperature structure of $Hg_3In_2\square Te_6$ is cubic with a point group either $\bar{4}3m$, $m\,3m$, or 432 with a lattice parameter of 18.870 ± 0.003 Å.[15] The compound has a zinc-blende superlattice comprised of $3\times 3\times 3$ zinc-blende cubes. The tellurium atoms lie on one zinc-blende sublattice; the

TABLE I. Elastic stiffness constants of vacancy compounds and those of the tetrahedrally bonded compounds HgTe and $CdGeAs_2$. Units are 10^{10} N m^{-2}.

	HgTe[a]	$Hg_5In_2\square Te_8$[b]	$Hg_3In_2\square Te_6$[c]	$HgIn_2\square Te_4$[d]	$Hg_5Ga_2\square Te_8$[e]	$Hg_3Ga_2\square Te_6$[d]	$CdGeAs_2$[f]
Elastic stiffness constants							
C_{11}	5.8	5.02	4.33	4.31	4.97	4.55	9.80
C_{12}	4.04	3.33	2.64	2.54	3.14	2.49	6.05
C_{13}				2.18			5.96
C_{33}				4.47			8.66
C_{44}	2.21	2.08	1.99	2.14	2.18	2.14	4.32
C_{66}				2.41			4.23
Bulk modulus							
B	4.62	3.89	3.20	2.99	3.75	3.18	7.10
$\frac{\frac{1}{2}(C_{11}-C_{12})}{B}$	0.19	0.22	0.26	0.29	0.24	0.32	0.26
C_{44}/B	0.48	0.53	0.62	0.72	0.58	0.67	0.61
Anisotropy ratio							
$\frac{2C_{44}}{(C_{11}-C_{12})}$	2.51	2.46	2.36	2.41	2.38	2.08	2.30

[a] Reference 10.
[b] Reference 13.
[c] Reference 5.
[d] Reference 6.
[e] Reference 14.
[f] Reference 12.

216-site-cell cube contains 18 molecules of $Hg_3In_2\Box Te_6$ and so includes 18 vacant lattice sites. MacKinnon *et al.*[3] pointed out that this information is compatible only with the space group $P\bar{4}3m$. Although their further explorations of the structure led to more useful information, including two possible configurations for the vacancies, the detailed atomic arrangements of the mercury, indium, and vacancies remain unresolved. The simple constraint that the average valency of the nearest neighbors of a given atom ought to be the same as in the parent zinc-blende compound is consistent with only two possible environments for tellurium atoms, namely (Hg, Hg, Hg, Hg) and (Hg, In, In, □), but this is not entirely compatible with the known symmetry.

Laue back-reflection x-ray photographs of single crystals and Debye-Scherrer powder photographs show that $Hg_5Ga_2\Box Te_8$ also consists of a zinc-blende superlattice in this case comprising $2\times2\times2$ zinc-blende cells with a lattice parameter of 12.472 ± 0.004 Å.[14] The tellurium atoms occupy the 32 *B* sites of this 64-site cell, which contains four molecules of $Hg_5Ga_2\Box Te_8$ and thus four vacancies. The powder lines of $Hg_5Ga_2\Box Te_8$ are the same as those of $Hg_5In_2\Box Te_8$, whose structure has been established by McCartney[9]—the Hg and In atoms are randomly distributed while the vacancies are ordered.

The structure of $HgIn_2\Box Te_4$ was determined by Saunders and Seddon and is drawn in Fig. 1 of their paper[6]; it is body-centered tetragonal with the symmorphic space group $I\bar{4}2m$. The c/a ratio has the ideal value of 2.00 and the lattice parameter a is 6.206 ± 0.002 Å. Miller *et al.*[2] point out that this is a defect stannite structure. It can be regarded as two adjacent zinc-blende cubes in which the atomic arrangements are very similar. The stacking is *ABCDEBCDA* along the *c* axis, where the planes *A* and *E* both contain mercury and vacant sites in the same arrangement but opposite positions; *B* and *D* are the tellurium planes and *C* the indium planes.[6] In a cubic crystal $C_{11}=C_{33}$, $C_{12}=C_{13}$, and $C_{44}=C_{66}$. The elastic constants of $HgIn_2\Box Te_4$ pair off: $C_{11}\sim C_{33}, C_{12}\sim C_{13}$ and $C_{44}\sim C_{66}$ (Table I). This pseudocubic elastic behavior has been visually depicted by recourse to cross sections of the ultrasonic-wave velocity and Young's-modulus surfaces.[6]

The hydrostatic pressure dependence of sufficient mode velocities were measured to obtain complete sets of the pressure derivatives of the elastic constants of $Hg_5Ga_2\Box Te_8$, $Hg_3In_2\Box Te_6$, and $HgIn_2\Box Te_4$. Ultrasonic-wave velocities were measured by a pulse-echo technique with a sensitivity of better than 1 part in 10^5 at pressures up to about 10^8 Pa in a piston and cylinder apparatus with the use of castor oil as the liquid pressure medium.[16] To account for the changes in crystal dimensions and density with pressure, the "natural velocity" W method[17] was used, the experimental data for pressure-induced change in pulse-echo-overlap frequency being converted to relative change of natural velocity $\Delta W/W_0$. The measured effects of hydrostatic pressure on the velocity of ultrasonic modes propagated in each of the three compounds studied are shown in Figs. 1–3. With the exception of the small decrease with pressure of the $[1\bar{1}0]$ polarized shear mode propagated in the [110] direction in $Hg_5Ga_2\Box Te_8$, the velocities increase with pressure in the normal way.

As the first step in processing these experimental results, the hydrostatic pressure derivatives c'_{jkrs} of

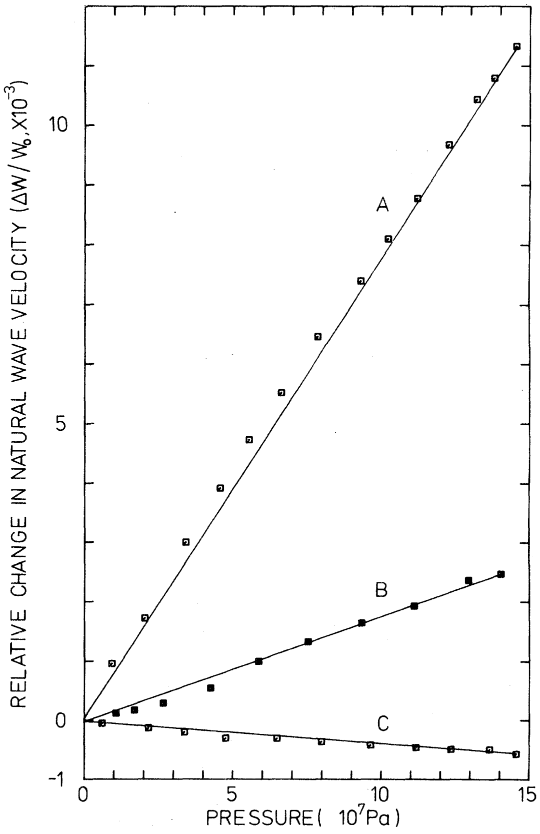

FIG. 1. Relative change in the "natural" wave velocity under hydrostatic pressure for $Hg_5Ga_2\Box Te_8$. The modes are *A*: $\underline{N}$[110], $\underline{U}$[110], *B*: $\underline{N}$[110], $\underline{U}$[001], *C*: $\underline{N}$[110], $\underline{U}[1\bar{1}0]$.

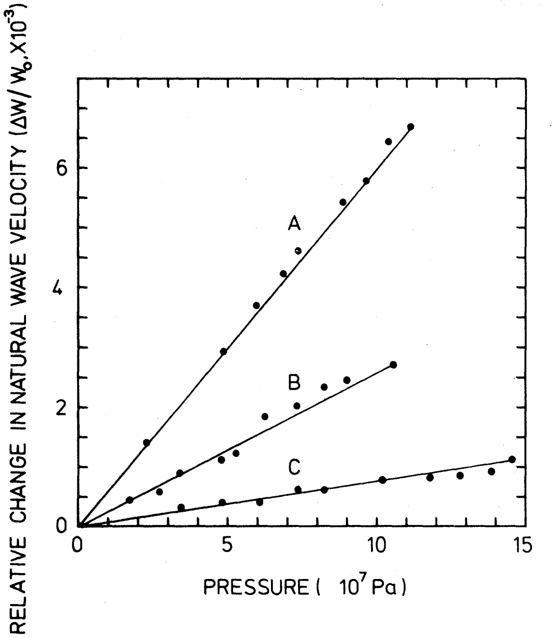

FIG. 2. Relative change in the "natural" wave velocity under hydrostatic pressure for $\mathrm{Hg_3In_2\square Te_6}$. The modes are *A*: $\underline{N}[110]$, $\underline{U}[110]$, *B*: $\underline{N}[110]$, $\underline{U}[001]$, *C*: $\underline{N}[110]$, $\underline{U}[1\bar{1}0]$.

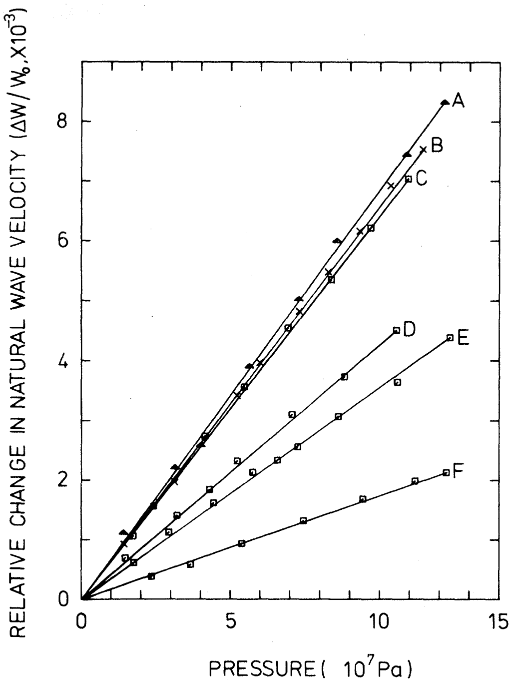

FIG. 3. Relative change in the "natural" wave velocity under hydrostatic pressure for $\mathrm{HgIn_2\square Te_4}$. The modes are *A*: $\underline{N}[100]$, $\underline{U}[100]$, *B*: $\underline{N}[0\,1/\sqrt{2}\,1/\sqrt{2}]$, $\underline{U}[0\,1/\sqrt{2}\,1/\sqrt{2}]$, *C*: $\underline{N}[110]$, $\underline{U}[110]$, *D*: $\underline{N}[100]$, $\underline{U}[001]$, *E*: $\underline{N}[100]$, $\underline{U}[010]$, *F*: $\underline{N}[0\,1/\sqrt{2}\,1/\sqrt{2}]$, $\underline{U}[0\,{-1}/\sqrt{2}\,1/\sqrt{2}]$.

the thermodynamic moduli have been obtained from the measured pressure gradient f' of the overlap frequency with the use of the following equation[18]:

$$2\rho_0 v_0^2 f'/f_0 = (\rho_0 W^2)'_{P=0} = -1 - U_j^0 U_k^0 (2\rho_0 v_0^2 S_{jkqq}^T - N_r N_s c'_{jrks}) \,. \tag{1}$$

Here the superscript 0 refers to parameters at atmospheric pressure, v_0 being the ultrasonic mode velocity and ρ_0 the density. N_i and U_i are direction cosines of the wave propagation and polarization directions, respectively. The explicit form of this relationship is determined by the crystal Laue group. For tetragonal 4/*mmm* (TI) Laue group crystals and in Voigt notation [writing B_{IJ} for c'_{ijkl} (Ref. 18)], it becomes

$$\begin{aligned}2\rho_0 v_0^2 f'/f_0 = & -1 - 2\rho_0 v_0^2[(S_{11}+S_{12}+S_{13})(U_1^2+U_2^2)+(2S_{13}+S_{33})U_3^2]+B_{11}(N_1^2U_1^2+N_2^2U_2^2)\\ & +2B_{12}N_1N_2U_1U_2+2B_{13}(N_1N_3U_1U_3+N_2N_3U_2U_3)+B_{33}N_3^2U_3^2\\ & +B_{44}[(N_2U_3+N_3U_2)^2+(N_1U_3+N_3U_1)^2]+B_{66}(N_1U_2+N_2U_1)^2 \,,\end{aligned} \tag{2}$$

from which the equations for cubic crystals can be readily obtained. The values of B_{IJ} are calculated from the hydrostatic pressure data given in Figs. 1–3 and are collected in Table II.

For crystals belonging to the 4/*mmm* (TI) Laue group, the effective pressure derivatives $\partial C_{IJ}/\partial P$ are related to the values of the thermodynamic quantities B_{IJ} by

$$\frac{\partial C_{11}}{\partial P} = B_{11} - 1 + (S_3 - 2S_1)C_{11} \,, \tag{3}$$

TABLE II. Hydrostatic pressure derivatives B_{IJ} of the thermodynamic second-order elastic constants (Ref. 18) of the vacancy compounds at 290 K.

B_{IJ}	$\mathrm{HgIn_2\square Te_4}$	$\mathrm{Hg_3In_2\square Te_6}$	$\mathrm{Hg_5Ga_2\square Te_8}$
B_{11}	7.61	7.53	7.35
B_{12}	4.58	4.79	5.12
B_{13}	4.56		
B_{33}	8.19		
B_{44}	3.40	2.46	2.24
B_{66}	3.49		

$$\frac{\partial C_{12}}{\partial P}=B_{12}+1+(S_3-2S_1)C_{12}\ , \tag{4}$$

$$\frac{\partial C_{13}}{\partial P}=B_{13}+1-S_3C_{13}\ , \tag{5}$$

$$\frac{\partial C_{33}}{\partial P}=B_{33}-1+(2S_1-3S_3)C_{33}\ , \tag{6}$$

$$\frac{\partial C_{44}}{\partial P}=B_{44}-1-S_3C_{44}\ , \tag{7}$$

$$\frac{\partial C_{66}}{\partial P}=B_{66}-1+(S_3-2S_1)C_{66}\ , \tag{8}$$

where

$$S_1=S_{11}+S_{12}+S_{13}$$

and

$$S_3=2S_{13}+S_{33}\ .$$

The corresponding equations for cubic crystals can be obtained by including the extra symmetry elements. The calculated values of $\partial C_{IJ}/\partial P$ for each crystal together with those of HgTe (Ref. 10) and $CdGeAs_2$ (Ref. 12) for comparison are given in Table III. It has been assumed throughout that the adiabatic and isothermal compressibilities are the same, the error introduced by this assumption into $\partial C_{IJ}/\partial P$ being less than 1%. An interesting feature of these results is that the pressure derivatives of the shear elastic constants C_{44} and C' $[=\frac{1}{2}(C_{11}-C_{12})]$ of the vacancy compounds have the normal positive sign. This is in direct contrast to the behavior of the tetrahedrally coordinated, zinc-blende-structure compound HgTe which shows anomalous negative values of $\partial C_{44}/\partial P$ and $\partial C'/\partial P$, indicative of the shear mode softening under pressure.

III. HYDROSTATIC PRESSURE EFFECTS ON THE ELASTIC BEHAVIOR OF VACANCY COMPOUNDS

The role played by the vacancies in determining the physical properties of the ordered vacancy compounds poses many intriguing problems. Much progress towards developing an understanding of the influence of vacancies on lattice-dynamical behavior has been made from optical studies of the zone-center optical-mode frequencies.[2–4,19] Ultrasonic-wave-velocity measurements determine the slope of the acoustic-mode, dispersion curves at the long-wavelength limit and their pressure dependences provide information on the shift of this slope, and thus of the change in mode vibrational energy, as the crystal is compressed. The central finding resulting from measurements of the second-order elastic constants of vacancy compounds in the mercury indium telluride and mercury gallium telluride series was that the bulk modulus decreases approximately linearly with increasing percentage of vacant sites.[5,6] Thus as the numbers of vacancies increase, the compounds become easier to compress. The experimental data for $\partial C_{IJ}/\partial P$ (Table III) for $Hg_5Ga_2\square Te_8$, $Hg_3In_2\square Te_6$, and $HgIn_2\square Te_4$ enable this feature of vacancy compounds to be extended to quantify the influence of hydrostatic pressure on crystal volume. The basic parameter which describes the behavior of a material under pressure is its compression: the ratio $V(P)/V_0$ of the volume $V(P)$ at pressure P to that V_0 at atmospheric pressure. Reliable values of the compression at pressures of more than an order of magnitude greater than those which are achievable in ultrasonic experiments can be obtained[20] by extrapolation based

TABLE III. Effective pressure derivatives $(\partial C_{IJ}/\partial P)$ at 290 K, elastic stiffness constants, and the pressure derivatives $(\partial B/\partial P)$ of the bulk moduli of $HgIn_2\square Te_4$, $Hg_3In_2\square Te_6$, $Hg_5Ga_2\square Te_8$ compared with those of HgTe and the chalcopyrite $CdGeAs_2$. $C'=\frac{1}{2}(C_{11}-C_{12})$.

$\partial C_{IJ}/\partial P$	$HgIn_2\square Te_4$	$Hg_3In_2\square Te_6$	$Hg_5Ga_2\square Te_8$	HgTe[a]	$CdGeAs_2$[b]
$\partial C_{11}/\partial P$	6.18	5.91	5.89	3.33	6.99
$\partial C_{12}/\partial P$	5.33	5.53	5.85	4.01	7.54
$\partial C_{13}/\partial P$	5.31				6.13
$\partial C_{33}/\partial P$	6.59				5.35
$\partial C_{44}/\partial P$	2.15	1.27	1.04	−0.12	−0.12
$\partial C_{66}/\partial P$	2.25				1.02
$\partial C'/\partial P$	0.43	0.19	0.017	−0.34	−0.27
$\partial B/\partial P$	5.64	5.66	5.86	3.78	6.18

[a] Reference 9.

[b] Reference 12.

on the Murnaghan equation of state[21]:

$$\frac{V(P)}{V_0}=\left[1+\frac{B_0'P}{B_0}\right]^{-1/B_0'} . \qquad (9)$$

The computed compressions of the vacancy compounds and the parent zinc-blende compound HgTe in Fig. 4 show that the more vacant sites there are, the greater is the compression, that is, the larger the decrease in cell volume for a given hydrostatic pressure. HgTe undergoes a phase transition to the hexagonal cinnabar structure at about 16×10^8 Pa (Refs. 22–24, 10); $Hg_3In_2\Box Te_6$ transforms to a rocksalt structure at 46×10^8 Pa.[8] Therefore, the compression curves in Fig. 4 have been terminated at the limits of stability of the atmospheric pressure forms of these two compounds.

Collapse to a denser modification is a feature common to many tetrahedrally coordinated sp^3 hybridized compounds with the diamond, zinc-blende, or chalcopyrite structures. In the context of valence force-field models, such crystals are considered to be stabilized against shear stresses by the interatomic forces required to bend the bonds. The elastic constants relate directly to these bond-bending and -stretching forces. A recent critical survey of the application of valence force field and related models to the diamond-structure elements has shown that such models are unable to account quantitatively for the internal strain even in the covalent semiconductors.[25] Thus, a valence force-field model is bound to be of limited value for ternary vacancy compounds. However, useful assessments of the bond-bending and -stretching force constants can be made from experimental data for vibrational-mode frequencies and the elastic constants. The zone-center, optical-vibrational modes of $HgIn_2\Box Te_4$ have been examined using Raman scattering and infrared-reflectivity measurements.[2] These data, together with those for the ultrasonic-wave velocities,[6] have been fitted[2] semiempirically to an adjustable force-constant model[26,27] of the Keating-Martin type. The particular value of this approach is that the model can be adapted to include bond-stretching force constants α for each type of bond in the crystal and bond-bending force constants β for each different triad of nearest-neighbor atoms. The Keating model parameters obtained are (i) bond stretching α: Hg-Te, 38.9; In-Te, 21.8; □-Te, 11.8, and (ii) bond bending β: In-Te-In, 2.95; In-Te-Hg, 2.95; Te-In-Te, 2.95; Te-Hg-Te, 2.95; □-Te-In, 1.47; □-Te-Hg, 1.47; Te-□-Te, 0.0.[2] To fit the phonon spectrum, it is necessary to incorporate a □-Te force constant (which implies that the vacancy represents not an empty site but a positive potential which attracts valence electrons from the four surrounding anions[2,4]). In spite of the physical difficulties associated with this model, especially in how the vacancy is to be treated, it provides a valuable guide to the relative magnitudes of the bond-bending and -stretching force constants.

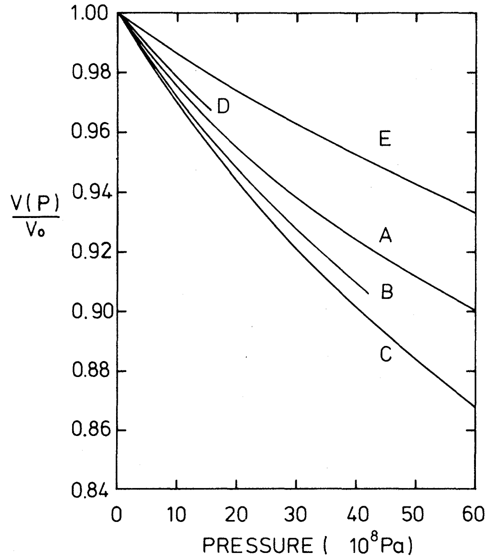

FIG. 4. The compression $V(P)/V_0$ of the vacancy compounds *A*: $Hg_5Ga_2\Box Te_8$, *B*: $Hg_3In_2\Box Te_6$, *C*: $HgIn_2\Box Te_4$ in comparison with that of *D*: HgTe and *E*: $CdGeAs_2$.

The stability of tetrahedrally bonded compounds is related to the ratio (β/α) of the bond-bending to -stretching force constants. An estimate of the ratio β/α (mean values of β and α will be assumed for the different force constants for the ternary vacancy compounds) can be arrived at by using the Keating[26] valence-force-field model from which the elastic constants can be related to the second-order Keating force constants α and β by

$$\begin{aligned}C_{11}&=(\alpha+3\beta)/a-4.053(Z^2q^2/a^4)\ ,\\ C_{12}&=(\alpha-\beta)/a-5.538(Z^2q^2/a^4)\ , \qquad (10a)\\ C_{44}&=(\alpha+\beta)/a-5.538(Z^2q^2/a^4)\\ &\quad-[(\alpha+\beta)/a-4.189(Z^2q^2/a^4)]\zeta^2\ .\end{aligned}$$

Here a is the lattice parameter. The second term on the right-hand side in each expression corresponds to the long-range electrostatic contribution expected for a mixed ionic-covalent crystal of ionicity Z.[27] In this model the internal strain parameter ζ is given by

$$\zeta=\frac{(\alpha-\beta)/a-10.058(Z^2q^2/a^4)}{(\alpha+\beta)/a-4.189(Z^2q^2/a^4)} . \quad (10b)$$

Values of the bond-bending to -stretching force constants ratio (β/α) for a number of zinc-blende compounds at atmospheric pressure and at the densification phase-transition pressure P_t calculated on this basis from elastic-constant measurements can be found in Table 5 of Ref. 28. In fact, the electrostatic contributions to the elastic constants are quite small, so that to a reasonable approximation C_{11} is $(\alpha+3\beta)/a$, C_{12} is $(\alpha-\beta)/a$, and C_{44} is $(\alpha+\beta)/a$. Thus $\frac{1}{2}(C_{11}-C_{12})/B$ is approximately equal to $2\beta/\alpha$ and C_{44}/B to $(\alpha+\beta)/\alpha$. These expressions have been tested for a number of zinc-blende compounds; for example, for HgTe the measured value of $\frac{1}{2}(C_{11}-C_{12})/B$ is 0.20,[10] while $2\beta/\alpha$, calculated with the use of the full Keating-Martin expressions (10), is 0.186. So $\frac{1}{2}(C_{11}-C_{12})/B$ provides a reasonable assessment of (twice) the ratio of the bond-bending to -stretching force constants. For the zinc-blende compounds $\frac{1}{2}(C_{11}-C_{12})/B$ ranges between 0.17 for HgTe and 0.28 for GaSb, while C_{44}/B falls between 0.45 for HgTe and 0.57 for GaSb.[28] Inspection of the values of $\frac{1}{2}(C_{11}-C_{12})/B$ and C_{44}/B given in Table I shows that the relative ease of bond bending to bond stretching in the vacancy compounds closely resembles that for the zinc-blende compounds. For a cubic crystal the anisotropy of the response to shear is expressed by the anisotropy factor $2C_{44}/(C_{11}-C_{12})$, which ranges between 2.51 for HgTe and 2.04 for GaSb for the zinc-blende compounds; the elastic anisotropy of the vacancy compounds is similar to that of the parent compound HgTe (Table I).

The densification transition undergone by zinc-blende-structure crystals at high pressures occurs when $\frac{1}{2}(C_{11}-C_{12})/B$ has reduced to a critical value of about 0.2 at the phase-transition pressure P_t (Refs. 10, 11, and 28). Since $\frac{1}{2}(C_{11}-C_{12})/B$ $\sim 2\beta/\alpha$, this stability criterion is equivalent to the force-constant ratio β/α falling to below about 0.1 when the crystal can no longer withstand bond-bending forces. C_{44}/B also tends to a critical value of 0.5 for the zinc-blende compounds at P_t. For the chalcopyrite $CdGeAs_2$ measurements of the elastic constants and their pressure derivatives have shown[12] that for this compound also, $\frac{1}{2}(C_{11}-C_{12})/B$ decreases to 0.15 and C_{44}/B to 0.39 at P_t [$\sim 60\times 10^8$ Pa (Ref. 29)]. Clearly it is of interest to find out whether the vacancy compounds behave similarly. With the use of the elastic constants (Table I) and their pressure derivatives (Table III), the pressure dependences of $\frac{1}{2}(C_{11}-C_{12})/B$ and C_{44}/B have been calculated; results are plotted in Fig. 5. Since the bulk modulus B increases more rapidly with pressure than the shear moduli, both $\frac{1}{2}(C_{11}-C_{12})/B$ and C_{44}/B decrease, like those of zinc-blende compounds[10,28] or $CdGeAs_2$,[12] with pressure. The parent compound HgTe collapses under pressure at about 15.5×10^8 Pa, when $\frac{1}{2}(C_{11}-C_{12})/B$ is 0.17 and C_{44}/B is 0.45.[10] It is interesting to observe that $Hg_3In_2\square Te_6$ undergoes its transition to a denser rocksalt form at 46×10^8 Pa (Ref. 8) when $\frac{1}{2}(C_{11}-C_{12})/B$ has fallen to 0.16 and C_{44}/B to 0.44. Thus it is likely that the transition in $Hg_3In_2\square Te_6$ results when the relative resistance to shear as against compression has fallen to a critical level, and the densification collapse, like that in zinc-blende, diamond, and chalcopyrite-structure compounds, is associated with softening of transverse-acoustic (TA) phonon modes. The remarkable correspondence at P_t between the values of $\frac{1}{2}(C_{11}-C_{12})/B$ and C_{44}/B for both HgTe and $Hg_3In_2\square Te_6$ suggests closely similar phase-transition mechanisms, even though $Hg_3In_2\square Te_6$ goes to a rocksalt form while HgTe transforms to the cinnabar structure (which can be thought of as a distorted rocksalt structure). It has been suggested[10] that the topotaxy of the phase transition in HgTe involves vector displacement of atoms on (110) planes with shear components corresponding to contributions from both $\frac{1}{2}(C_{11}-C_{12})$ and C_{44} modes; such a mechanism can lead to either the rocksalt or cinnabar structures. If this mechanism were to be generally followed by tetrahedrally bonded structures, then the stability criterion that $\frac{1}{2}(C_{11}-C_{12})/B$ reach a critical value at P_t could be used to predict phase-transition pressures. The results for HgTe and $Hg_3In_2\square Te_6$ show that the critical value in those compounds is close to 0.17. The ratio $\frac{1}{2}(C_{11}-C_{12})/B$ should fall to this value at 40×10^8 Pa for $Hg_5Ga_2\square Te_8$ (Fig. 5) and 70×10^8 Pa for $HgIn_2\square Te_4$ at which pressures these compounds may undergo densification transitions yet to be observed. The occurrence at 42×10^8 Pa of a transition in $Hg_5In_2\square Te_8$ (Ref. 8) is consistent with this suggestion.

The phase transitions in $Hg_5In_2\square Te_8$ at 42×10^8 Pa and in $Hg_3In_2\square Te_6$ at 46×10^8 Pa (Ref. 8) take place at much higher pressure than that ($\sim 16\times 10^8$ Pa) in HgTe itself. At first sight this is surprising because the compressions of the vacancy compounds are larger than that of HgTe

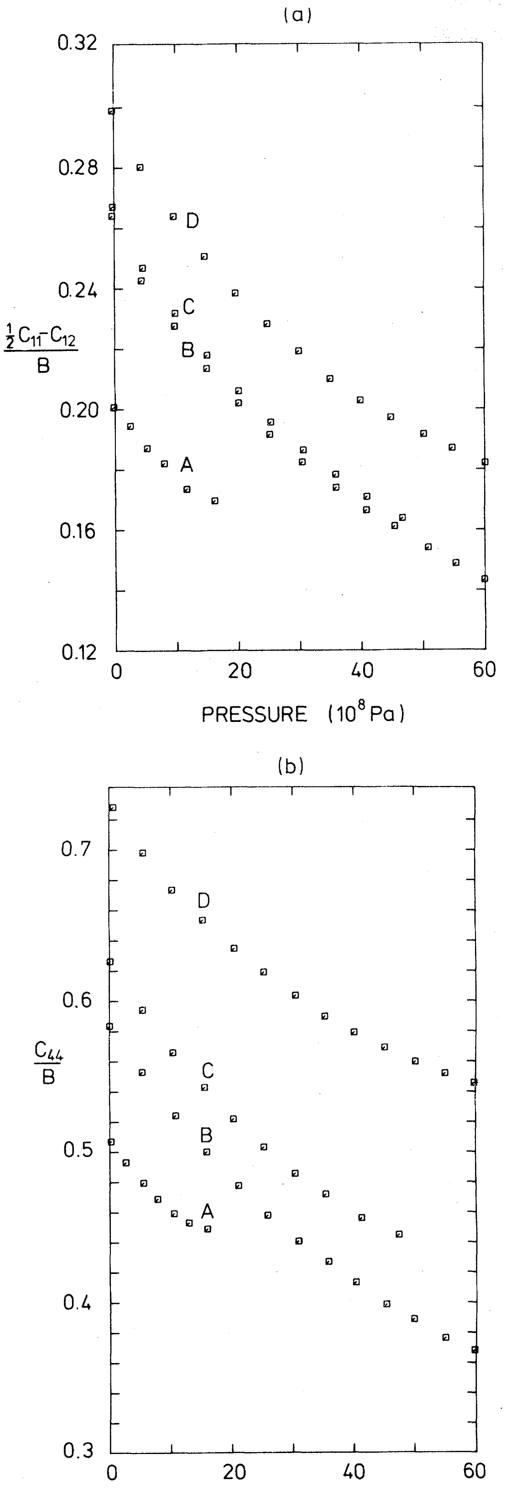

FIG. 5. Effect of hydrostatic pressure on the shear to bulk modulus ratio for vacancy compounds (a) $\frac{1}{2}(C_{11}-C_{12})/B$ and (b) C_{44}/B. *A*: HgTe, *B*: $Hg_5Ga_2\square Te_8$, *C*: $Hg_3In_2\square Te_6$, *D*: $HgIn_2\square Te_4$.

(Fig. 4) and the phase changes are to denser structures. However, this apparent paradox can be resolved by reference to the pressure-derivative measurements of the elastic constants (Table III). The elastic behavior of HgTe is anomalous in that both the shear elastic constants $\frac{1}{2}(C_{11}-C_{12})$ and C_{44}, which are small compared with the bulk modulus even at atmospheric pressure, decrease under hydrostatic pressure. The negative signs of the pressure derivatives $\partial[\frac{1}{2}(C_{11}-C_{12})]/\partial P$ and $\partial C_{44}/\partial P$ show that all the transverse-acoustic modes soften at the Brillouin-zone center when HgTe is subjected to hydrostatic pressure. This shear-mode softening enhances the reduction in $\frac{1}{2}(C_{11}-C_{12})/B$ and C_{44}/B, so that this zinc-blende compound undergoes the phase transition at a comparatively low pressure when the stabilization against shear stresses by bond-bending forces reaches too low a level. Bond bending is a change in the angle between sp^3 hybrid orbitals and can be considered to be a mixing of the sp^3 wave functions with others of *d* and *f* symmetry.[30,31] For a heavy element compound like HgTe, the promotion energy for electrons from sp^3 orbitals to the next unfilled *d* and *f* levels is small, and the high ionicity of II-VI compounds further reduces the energy needed to bend the bonds. Thus in HgTe the bond-bending force constant β is particulary small ($2.31\ \mathrm{N\,m^{-1}}$).[10] Under pressure, the bond-stretching force constant α increases (from 28.2 $\mathrm{N\,m^{-1}}$ at atmospheric pressure to 29.7 $\mathrm{N\,m^{-1}}$ at 15.5×10^8 Pa—just below P_t), while β decreases. Now the effect of pressure on the elastic properties of the vacancy compounds is quite different. In each case $\partial[\frac{1}{2}(C_{11}-C_{12})]/\partial P$ and $\partial C_{44}/\partial P$ are small but positive (Table III): The anomalous shear-mode softening observed in HgTe [and in other zinc-blende compounds such as HgSe (Ref. 11)] is conspicuously absent (except to a small extent in $Hg_5Ga_2\square Te_8$, Fig. 1). The decrease of the ratios $\frac{1}{2}(C_{11}-C_{12})/B$ and C_{44}/B with pressure, discussed earlier, is due to the fact that $\partial B/\partial P$ is larger than either $\partial[\frac{1}{2}(C_{11}-C_{12})]/\partial P$ or $\partial C_{44}/\partial P$. Hence the lack of shear-mode softening with pressure ensures that the ratios $\frac{1}{2}(C_{11}-C_{12})/B$ and C_{44}/B achieve the critical values for shear instability at higher pressures for the vacancy compounds than for HgTe.

This influence of the sited vacancies on the behavior of the shear acoustic modes with pressure needs to be considered further. The effect of pressure on the individual vibrational modes can be quantified by consideration of the acoustic-mode-

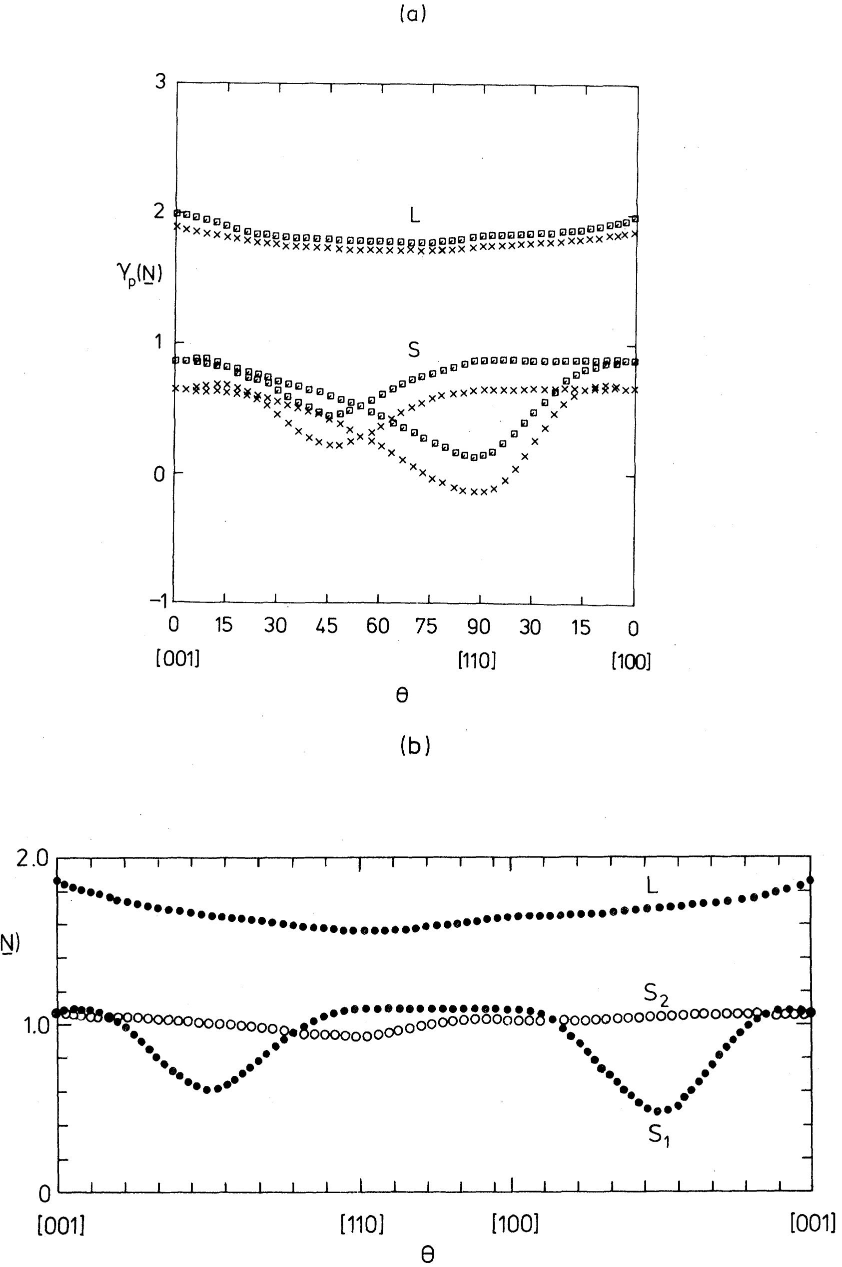

FIG. 6. Acoustic-mode-Grüneisen gammas in the long-wavelength limit for (a) $Hg_5Ga_2\Box Te_8$, and $Hg_3In_2\Box Te_6$ and (b) $HgIn_2\Box Te_4$ as a function of orientation (angle θ). In (a) the crosses refer to $Hg_5Ga_2\Box Te_8$ and the squares to $Hg_3In_2\Box Te_6$. The upper pair of curves show the mode gammas for quasilongitudinal modes, and the lower four curves are for quasishear modes.

Grüneisen parameters at the long-wavelength limit. These specify the isothermal strain dependence of the lattice-vibration frequency $\omega_p(\vec{N})$ of a mode of polarization index p $(=1,2,3)$ and with a unit vector $\vec{N}$ in the direction of propagation.[32,33] At ultrasonic frequencies the wavelength is so long that use of the elastic continuum model is entirely satisfactory. The method of obtaining the acoustic-mode-Grüneisen parameters has been detailed by Brugger and Fritz,[33] and its extension to tetragonal $4/mmm$ (TI) Laue group crystals given recently.[12] With the use of the elastic constants (Table I) and their pressure derivatives (Tables II and III) as the input data, the acoustic-mode-Grüneisen parame-

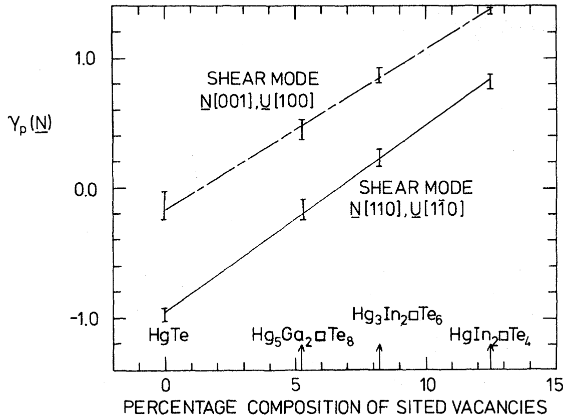

FIG. 7. Mode-Grüneisen gammas for the two pure shear waves $\underline{N}[100]$, $\underline{U}[001]$ and $\underline{N}[110]$, $\underline{U}[1\bar{1}0]$ as a function of the percentage of sited vacancies.

ters in the symmetry planes of the vacancy compounds have been computed (Fig. 6). Normally, mode-Grüneisen parameters are positive: The crystal energy and thus the vibrational frequencies are expected to increase with pressure. Application of pressure leads to a small anomalous reduction in the velocity of the [110], polarization [1$\bar{1}$0] shear mode in $Hg_5Ga_2\square Te_8$ (Fig. 1): This mode softens slightly. With this exception, the acoustic modes in vacancy compounds show normal behavior. To clarify the influence of ordered vacancies on the shear-mode behavior with pressure, the Grüneisen parameters for the [110], polarization [1$\bar{1}$0] and of the [001], polarization [100] shear modes, which correspond to the shear moduli $\frac{1}{2}(C_{11}-C_{12})$ and C_{44}, respectively, in both cubic and tetragonal crystals, have been plotted in Fig. 7. For these two shear modes, the Grüneisen parameters can be expressed as

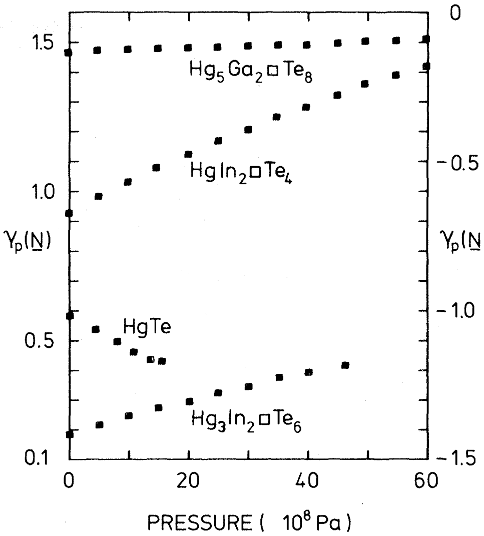

FIG. 8. Effect of hydrostatic pressure on the mode-Grüneisen gammas $\gamma_p(\vec{N})$ for the $\underline{N}[110]$, $\underline{U}[1\bar{1}0]$ shear mode. The $\gamma_p(\vec{N})$ for this mode are negative for HgTe and $Hg_5Ga_2\square Te_8$ (values given by the scale on the right-hand ordinate) but positive for $Hg_3In_2\square Te_6$ and $HgIn_2\square Te_4$ (values on the left-hand ordinate).

$$ {}_H\gamma_S^T(\vec{N}) = -\frac{B}{2}\left[S_3 - \frac{1}{C}\frac{\partial C}{\partial P} \right] . \tag{11}$$

Thus the sign of ${}_H\gamma_S^T(\vec{N})$ is determined by the sum of the linear compressibility S_3 along the fourfold axis and $-(1/C)(\partial C/\partial P)$ [where C is either $\frac{1}{2}(C_{11}-C_{12})$ or C_{44}]. For a tetragonal crystal belonging to the $4/mmm$ Laue group, Eq. (11) becomes

$$ {}_H\gamma_{[001]}^T[100] = -\left[\frac{C_{11}+C_{12}-2C_{13}}{2C_{11}+2C_{12}+4C_{33}-8C_{13}} - \frac{(C_{11}C_{33}+C_{12}C_{33}-2C_{13}^2)}{2C_{44}(C_{11}+C_{12}+2C_{33}-4C_{13})}\frac{\partial C_{44}}{\partial P} \right] \tag{12}$$

and

$$ {}_H\gamma_{[1\bar{1}0]}^T[110] = -\left[\frac{C_{11}+C_{12}-2C_{13}}{2C_{11}+2C_{12}+4C_{33}-8C_{13}} - \frac{(C_{11}C_{33}+C_{12}C_{33}-2C_{13}^2)}{(C_{11}-C_{12})(C_{11}+C_{12}+2C_{33}-4C_{13})}\frac{\partial[\frac{1}{2}(C_{11}-C_{12})]}{\partial P} \right] . \tag{13}$$

Reappearance of the ratios $\frac{1}{2}(C_{11}-C_{12})/B$ and C_{44}/B in the explicit forms of Eq. (11) for the shear-mode gammas ${}_H\gamma_{[1\bar{1}0]}^T[110]$ and ${}_H\gamma_{[001]}^T[100]$ is consistent with the conclusions about the relationships between crystal stability, force-constant ratio β/α, and shear-mode softening. The origin of the sign of the shear-mode-Grüneisen parameter can be seen directly from Eq. (11): The small negative value of ${}_H\gamma_{[1\bar{1}0]}^T[110]$ for $Hg_5Ga_2\square Te_8$ (Fig. 6) comes about because $\partial[\frac{1}{2}(C_{11}-C_{12})]/\partial P$ is less than $\frac{1}{2}(C_{11}-C_{12})/3B$. The linear increase of the two shear-mode-Grüneisen parameters with increasing concentration of sited vacancies (Fig. 7) shows that vacancies additively inhibit shear-mode softening. The effect of hydrostatic pressure on the Grüneisen gammas for what is the softest shear mode in the zinc-blende compounds, namely that associated with $\frac{1}{2}(C_{11}-C_{12})$, is shown in Fig. 8 for the vacancy compounds. While pressure induces further softening of this mode in HgTe, the mode frequency ω_p is increased for $HgIn_2\square Te_4$ and $Hg_3In_2\square Te_6$. For $Hg_5Ga_2\square Te_8$ the slightly negative shear-mode-Grüneisen gamma is almost constant with pressure.

The thermodynamic Grüneisen function γ^{th} $(=\beta V B_S/C_p)$ (where β is the volume-expansion coefficient) of tetrahedrally bonded elements and compounds has a minimum value at a temperature of about $0.07\Theta_0$ [where Θ_0 is the limiting value of the Debye characteristic temperature as temperature $\rightarrow 0$ K (Refs. 34–36)]. The limiting value γ_0^{th} of the Grüneisen parameter of HgTe is -1.2 ± 0.2.[36] At low temperatures, the soft [110], polarization [1$\bar{1}$0] is the most easily excited lattice mode, and the γ_i for this mode (and also those for all the other shear modes in HgTe) is negative[10]; hence the contributions of these γ_i will result in a negative value for the weighted average γ^{th}—the thermal expansion is then negative.[36–38] However, for the vacancy compounds, the shear-mode-Grüneisen parameters are positive (with the exception of that for the [110], polarization [1$\bar{1}$0] shear mode for $Hg_5Ga_2\square Te_8$), which suggests that the thermal expansions of these compounds should not show the anomalous negative values at low temperature, which is characteristic of other tetrahedrally bonded crystals.

On average, in $Hg_5Ga_2\square Te_8$ there is one vacancy attached to two tellurium atoms, and in $Hg_3In_2\square Te_6$ there are two vacancies for every three tellurium atoms, while in $HgIn_2\square Te_4$ every tellurium atom is adjacent to a vacancy. As the vacancy concentration increases, the sp^3-hybrid orbital description of the bonding must become progressively less adequate. A tentative explanation of the effects of pressure on the elastic behavior of the vacancy compounds is as follows. In HgTe itself where the bonding is mixed ionic sp^3 hybrid covalent in character, as the pressure is increased, the ionicity is enhanced and so the shear modes soften.[10] But in the vacancy compounds the four Te atoms adjacent to a vacancy can be expected to have relaxed outwards—the hybridization shifts from sp^3 towards sp^2 and the ionicity should be somewhat enhanced. Now increasing pressure forces the tellurium atoms in towards the center of vacancy: Hence the high compressibility of these vacancy compounds. This process will take the hybridization closer towards sp^3, decreasing the ionicity and leading the stiffening of the shear modes.

ACKNOWLEDGMENTS

We are grateful to J. Penfold and Dr. G. D. Pitt for allowing us the use of the SERC high-pressure facilities centered at STL Harlow and to the SERC for financial support. We would also like to thank R. C. J. Draper and E. F. Lambson for experimental assistance and Dr. D. W. Bullett for many useful discussions.

---

[1] E. Parthe, *Crystal Chemistry of Tetrahedral Structures* (Gordon and Breach, New York, 1964).

[2] A. Miller, D. J. Lockwood, A. MacKinnon, and D. Weaire, J. Phys. C 9, 2997 (1976).

[3] A. MacKinnon, A. Miller, D. J. Lockwood, G. Ross, and G. D. Holah, in *Ternary Compounds,* edited by G. D. Holah (IOP, London, 1977), p. 119.

[4] A. Miller, A. MacKinnon, and D. Weaire, in *Solid State Physics,* edited by H. Ehrenreich, F. Seitz, and D. Turnbull (Academic, New York, 1981), Vol 36, p. 119.

[5] G. A. Saunders and T. Seddon, J. Phys. Chem. Solids 31, 2495 (1970).

[6] G. A. Saunders and T. Seddon, J. Phys. Chem. Solids 37, 873 (1976).

[7] R. W. Keyes, J. Appl. Phys. 33, 3371 (1962).

[8] G. D. Pitt, J. H. McCartney, J. Lees, and D. A. Wright, J. Phys. D 5, 1330 (1972).

[9] J. H. McCartney, Ph.D. thesis, University of London, 1970 (unpublished).

[10] A. J. Miller, G. A. Saunders, Y. K. Yoḡurtçu, and A. E. Abey, Philos. Mag. 43, 1447 (1981).

[11] P. J. Ford, A. J. Miller, G. A. Saunders, Y. K. Yoḡurtçu, J. K. Furdyna, and M. Jaczynski, J. Phys. C 15, 657 (1982).

[12] Tu Hailing, G. A. Saunders, W. A. Lambson, and R. S. Feigelson, J. Phys. C 15, 1399 (1982).

[13] T. Alper, N. G. Pace, and G. A. Saunders, Br. J. Appl. Phys. 1, 1079 (1968).

[14] G. A. Saunders and T. Seddon, Phys. Lett. 34A, 443

(1971).

[15] C. A. Maynell, G. A. Saunders, and T. Seddon, Phys. Lett. 31A, 338 (1970).

[16] Y. K. Yoğurtçu, A. J. Miller, and G. A. Saunders, J. Phys. C 13, 6585 (1980).

[17] R. N. Thurston and K. Brugger, Phys. Rev. 133, A1604 (1964).

[18] R. N. Thurston, Proc. IEEE 53, 1320 (1965).

[19] A. Miller, A. MacKinnon, D. L. Weaire, C. R. Pidgeon, D. J. Lockwood, and G. A. Saunders, in *Proceedings of the XIII International Conference of the Physics of Semiconductors, Rome, 1976,* edited by F. G. Fumi (North-Holland, Amsterdam, 1976), p. 509.

[20] O. L. Anderson, J. Phys. Chem. Solids 27, 547 (1966).

[21] F. D. Murnaghan, Proc. IEEE 53, 1320 (1965).

[22] P. W. Bridgman, Proc. Am. Acad. Arts Sci. 74, 21 (1940).

[23] A. Jayaraman, W. Klement, and G. C. Kennedy, Phys. Rev. 130, 2277 (1963).

[24] T. M. Turusbekov and E. I. Estrin, Fiz. Tverd. Tela (Leningrad) 21, 951 (1979) [Sov. Phys.—Solid State 21, 558 (1979)].

[25] C. Cousins, J. Phys. C 15, 1857 (1982).

[26] P. N. Keating, Phys. Rev. 149, 674 (1966).

[27] R. M. Martin, Phys. Rev. B 1, 4005 (1970).

[28] Y. K. Yoğurtçu, A. J. Miller, and G. A. Saunders, J. Phys. Chem. Solids 42, 49 (1981).

[29] H. Katzman, T. Donohue, W. F. Libby, and H. L. Luo, J. Phys. Chem. Solids 30, 2794 (1969).

[30] J. C. Philips, Rev. Mod. Phys. 42, 317 (1970).

[31] J. C. Philips, *Bonds and Bands in Semiconductors* (Academic, New York, 1973).

[32] K. Brugger, Phys. Rev. 133, A1611 (1964).

[33] K. Brugger and T. C. Fritz, Phys. Rev. 157, 524 (1967).

[34] P. W. Sparks and C. A. Swenson, Phys. Rev. 163, 779 (1967).

[35] T. H. K. Barron, J. A. Birch, and G. K. White, J. Phys. C 10, 1617 (1977).

[36] J. G. Collins, G. K. White, J. A. Birch, and T. F. Smith, J. Phys. C 13, 1649 (1980).

[37] M. Blackman, Philos. Mag. 3, 831 (1958).

[38] A. Bienenstock, Philos. Mag. 9, 755 (1964).